1  *Removal of TcO₄⁻ from Representative Nuclear Waste Streams with Layered Potassium Metal*

2  *Sulfide Materials*

3  James J. Neeway,[*,†] R. Matthew Asmussen,[†] Amanda R. Lawter,[†] Mark E. Bowden,[‡] Wayne W.

4  Lukens,[§] Debajit Sarma,[ʃ] Brian J. Riley,[†] Mercouri G. Kanatzidis,[ʃ] Nikolla P. Qafoku[†]

5  [†]*Energy and Environment Directorate, Pacific Northwest National Laboratory, Richland, WA 99352,*

6  *USA*

7  [‡]*W.R. Wiley Environmental Molecular Sciences Laboratory, Pacific Northwest National Laboratory,*

8  *Richland, WA 99352, USA*

9  [§]*Chemical Sciences Division, Lawrence Berkeley National Laboratory, Berkeley, CA 94720, USA*

10  [ʃ]*Department of Chemistry, Northwestern University, Evanston, IL 60208, USA*

**Abstract:**

12  Many efforts have focused on the sequestration and immobilization of $^{99}$Tc because the

13  radionuclide is highly mobile in oxidizing environments and presents serious health risks due to

14  its radiotoxicity and long half-life ($t_{1/2}$ = 213 000 a). One of the more common methods for Tc

15  removal from solution and immobilization in solids is based on reducing Tc from highly soluble

16  Tc$^{(VII)}$ to sparingly soluble Tc$^{(IV)}$. In order to remove solution Tc through this reduction process,

17  the Tc-sequestering solid must contain a reducing agent and, ideally, the Tc-sequestering

18  material would function in a large range of chemical environments. For long-term stability, the

19  reduced Tc would preferentially be incorporated into the resulting mineral structure instead of

20  simply being sorbed onto the mineral surface. Here, we report results obtained from batch

21  sorption experiments performed in anoxic and oxic conditions with two sulfide-containing

1    potassium metal sulfide (KMS) materials, known as KMS-2 and KMS-2-SS. In deionized water

2    in anoxic conditions after 15 d of contact, KMS-2 is capable of removing ~45% of Tc and KMS-

3    2-SS is capable of removing ~90% of Tc. The improved performance of KMS-2-SS compared to

4    KMS-2 in deionized water in anoxic conditions appears to be linked both to a higher pH

5    resulting from the batch sorption experiments performed with KMS-2-SS and a higher overall

6    purity of KMS-2-SS. Both materials perform even better in highly caustic (pH~13.5), high ionic

7    strength (8.0 M) simulated Hanford low-activity waste solutions, removing more than 90% Tc

8    after 15 d of contact in anoxic conditions. Post-reaction solids analysis indicate that Tc(VII) is

9    reduced to Tc(IV) and that Tc(IV) is bonded to S atoms in the resulting KMS-2 structure in a

10    $Tc_2S_7$ form. In contrast to previous ion exchange experiments with other KMS materials, the

11    batch sorption experiments examining Tc removal cause the initially crystalline KMS materials

12    to lose much of their initial long-range order.

13

## 1    Introduction

2      The ^{99}Tc isotope is generated primarily during the fission of [235]U and [239]Pu. Due to its high

3      mobility in oxidizing environments, radiotoxicity, and long half-life ($t_{1/2}$ = 213 000 a),

4      management of ^{99}Tc in radioactive waste streams is of particular importance at nuclear reactors,

5      at nuclear fuel reprocessing facilities such as Sellafield, United Kingdom and La Hague, France,

6      and at legacy waste sites from Cold War activities situated around the world.[1-2] Additionally, the

7      inventory of ^{99}Tc is expected to grow if nuclear power generation is pursued by countries hoping

8      to increase their energy production without increasing their emission of greenhouse gases.

9      Therefore, ^{99}Tc management is important both in assisting in cleanup efforts of legacy waste

10     sites around the world and ensuring safe disposal of radioactive waste from power generation

11     from nuclear reactors.

12     At one existing legacy waste site, Hanford Site, in southeast Washington State, USA,

13     approximately 1.99 Mg of [99]Tc (or 1.25 PBq) was produced between 1943 and 1987.[3] The

14     majority of the ^{99}Tc at the site is located in single- and double-shell tanks containing mixed and

15     radioactive wastes and exists primarily as pertechnetate [$TcO_4^-$] (from this point forward, we will

16     refer to ^{99}Tc simply as Tc unless specifying the isotope is necessary in the discussion). Current

17     cleanup plans call for separating the tank waste into high-volume, low-activity waste (LAW) and

18     low-volume, high-level waste (HLW) fractions, which will be vitrified at separate facilities in a

19     borosilicate glass matrix. Before vitrification, the aqueous LAW fraction consists of a highly

20     caustic (~pH 13.5), high ionic strength aqueous solution containing $Na^+$ (5–10 M), $K^+$, $Al(OH)_4^-$,

21     $Cl^-$, $F^-$, $NO_2^-$, $NO_3^-$, $OH^-$, $CO_3^{2-}$, organics, and minor ionic species including dissolved metals

22     such as Cr, Ni, Cd, and Pb, and radionuclides. The majority of the ^{99}Tc is expected to partition to

23     the LAW fraction.[4] However, immobilization of Tc in the vitrified product is difficult because Tc

1    volatilizes at the high processing temperatures (~1150 °C) and has relatively low solubility in the

2    borosilicate glass matrix, ~2000 ppm to ~2800 ppm, depending on redox conditions.[5-6] It would,

3    therefore, be advantageous to find a material capable of removing the $TcO_4^-$ from the chemically

4    complex aqueous waste streams before vitrification and capable of immobilizing the Tc in a

5    durable low-temperature waste form for long-term disposal. However, separating the $TcO_4^-$ from

6    the complex aqueous LAW waste stream is particularly challenging due to its high pH and ionic

7    strength.

8    Two techniques that can remove $TcO_4^-$ from aqueous solutions are solvent extraction and

9    sorption (chemisorption and/or physisorption). Solvent extraction, such as the PUREX or UREX

10   processes, is based on an organic phase that strips the $TcO_4^-$ from the aqueous phase.[7-8] In the

11   case of sorption on a material surface, Tc removal is either through an ion exchange process[9-12]

12   or a reductive process whereby the sorbent reduces the highly soluble $Tc^{(VII)}O_4^-$ to a sparingly

13   soluble Tc(IV) form such as $Tc^{(IV)}O_2 \cdot nH_2O$ ($2.6 \times 10^{-9}$ M);[13] the associated redox reaction and

14   standard reduction potential is shown in Equation (1).[14]

15       $$TcO_4^- + 4\,H^+ + 3\,e^- \leftrightarrow TcO_2 + 2\,H_2O \qquad (E = 0.746 \pm 0.012\ V) \qquad (1)$$

16   A recent review of materials capable of removing Tc from solution identified several

17   materials that reductively separate Tc.[15] These materials include apatites,[12,16] metals such as

18   zinc[17] or iron,[18-20] iron-sulfides,[21] blast furnace slags,[22] chalcogels,[23] and activated carbon,[12,24-27]

19   The effectiveness of these materials is generally determined using batch sorption experiments in

20   anoxic environments. Other than a few studies,[21,27-28] the batch sorption tests are performed in

21   simulated groundwater solution with circumneutral pH and ionic strengths several orders of

22   magnitude lower than that of aqueous LAW. However, to understand the effectiveness of

1    materials to remove Tc from aqueous LAW, experiments must be performed at higher pH and

2    ionic strength in the presence of competing ions.

3        Layered metal sulfides have been reported to effectively adsorb soft cations through typical

4    ion exchange reactions. Inorganic potassium metal sulfides (KMS/KTS) have been reported to

5    extract both monovalent ($Cs^+$ and $Ag^+$) and divalent ($Sr^{2+}$, $Ni^{2+}$, and $Hg^{2+}$) soft-Lewis acid

6    cations from aqueous environments.[29-33] One KMS material, KMS-2, is composed of sheets of

7    edge-sharing (Mg/Sn)$S_6$ octahedra with intercalated $K^+$ ions, where Mg and Sn atoms occupy the

8    same crystallographic position and S atoms are three-coordinated.

9        Soft cations are extracted by KMS-2 via ion exchange of the interstitial $K^+$ by the cation of

10   concern. However, this material has not been studied for its ability to remove anions from

11   solution. The KMS-2 sorbent is particularly attractive for possible $TcO_4^-$ removal because of its

12   layered structure and high reductive capacity due to the presence of sulfide ions. The high

13   reductive capacity is desirable in materials that reductively sequester contaminants.

14       In this study, we demonstrate the effectiveness of $TcO_4^-$ removal by KMS-2-SS ($K_2MgSn_2S_6$)

15   and a novel carbonate-containing form of KMS-2, called KMS-2. Batch sorption tests were

16   performed in both deionized water (DIW) and a highly caustic, high ionic strength LAW

17   simulant to measure the effective of $TcO_4^-$ in two very different chemical environments. The

18   LAW simulant also contains redox-active species such as Cr(VI) and $NO_3^-$ that can interfere with

19   the removal of Tc from solution.[34] The competition of Cr with Tc has already been demonstrated

20   by other immobilizing agents targeting Tc.[35-36] Additionally, tests were performed under oxic

21   and anoxic conditions to examine the re-oxidation of Tc(IV) to Tc(VII) in the presence of

22   oxygen, as has been observed in other systems.[37] Post-reaction X-ray absorption spectroscopy

1 (XAS) were used to determine the Tc oxidation state using X-ray absorption near edge structure

2 (XANES) spectroscopy and the local environment of Tc was determined by X-ray absorption

3 fine structure (EXAFS) spectroscopy.. These analyses confirm the role of S (as $S^{2-}$) in Tc

4 removal. X-ray diffraction (XRD) of the pre- and post-reaction materials demonstrated that the

5 crystalline structure was modified during $TcO_4^-$ removal, which is in contrast to the simple ion-

6 exchange mechanism observed with cation removal by KMS materials.

7 **Experimental Section:**

8 **Synthesis of $K_{2x}Mg_xSn_{3-x}S_6$ ($x$ = 0.5-1) (KMS-2).** Hydrothermal synthesis: Elemental Sn (76

9 mmol, 9.0 g), Mg (38 mmol, 0.92 g), S (266 mmol, 8.5 g), $K_2CO_3$ (57 mmol, 7.9 g), were mixed

10 in a 23-ml Teflon-lined stainless-steel autoclave. Deionized water (3 mL) was added drop wise

11 until the mixture acquired dough-like consistency. The autoclave was sealed properly and soaked

12 in a preheated oven at 220°C for 15 h under autogenous pressure. Then, the autoclave was

13 allowed to cool at room temperature. A yellow polycrystalline product was isolated by filtration

14 (14.20 g, yield ~70% based on Sn), washed several times with water, acetone, and ether (in that

15 order), and dried under vacuum. Energy dispersive spectroscopy (EDS) analysis gave the

16 average formula " $K_{1.35}Mg_{0.6}Sn_{2.6}S_6$".

17 **Synthesis of $K_{2x}Mg_xSn_{3-x}S_6$ ($x$ = 0.5-1) (KMS-2-SS).** Solid-state synthesis: A mixture of Sn

18 (8.9 mmol, 1055 mg), Mg (4.7 mmol, 113 mg), $K_2S$ (4.6 mmol, 204 mg), and S (15.7 mmol, 512

19 mg) was sealed under vacuum ($10^{-4}$ Torr) in a fused silica tube and heated (10°C/h) to 550°C for

20 48 h, followed by cooling to room temperature at 100°C/h. The yellow polycrystalline product

21 obtained was washed several times with water, acetone, and ether (in that order) (2 g, ~ 85%

1    yield based on Sn). Energy dispersive spectroscopy (EDS) analysis gave the average formula

2    "$K_{1.3}Mg_{0.95}Sn_{2.1}S_6$".[30]

3    **Batch Sorption Experiments with KMS-2:** The effectiveness of $TcO_4^-$ removal by KMS-2 and

4    KMS-2-SS was investigated in 18.2 MΩ-cm deionized Millipore® water (DIW) and a LAW

5    simulant. The LAW simulant is based on the Hanford Tank Waste Operations Simulator

6    (HTWOS) model that supports the River Protection Project System Plan Revision 6.[38] The

7    average measured concentration of major elements of the LAW simulant is presented in Table 1.

8    The average measured pH of the LAW simulant was 13.5.

9    Table 1 –Measured concentration of major elements of LAW simulant used in tests. The average measured pH of

10   the LAW solution was 13.5.

| Constituent | Measured concentration (M) |
|-------------|----------------------------|
| Na          | 8.7                        |
| Al          | 0.55                       |
| Cr          | $3.5\times10^{-2}$         |
| Pb          | $4.3\times10^{-4}$         |
| NO3         | 2.5                        |
| NO2         | 0.29                       |
| SO4         | 0.12                       |
| Cl          | 0.12                       |

11

12       Batch sorption tests at ~22 °C involved placing 1.0 g of KMS-2 and KMS-2-SS in contact

13   with 100 mL of solution in a 250-mL polytetrafluoroethylene (PTFE) bottle at room temperature

14   for various durations with periodic solution sampling. Following addition of the DIW or LAW

15   simulant to the bottle, the solutions were spiked with a concentrated stock solution of NaTcO₄

16   (0.10 M) to achieve Tc concentrations of ~5.7 × $10^{-4}$ M, which is 10× the level predicted by

1    HTWOS. Periodic sampling was performed by pipetting a 2-mL aliquot of solution from the test

2    vessels which was immediately filtered (0.2 µm). The volume removed during sampling was not

3    replaced. Experiments were performed either in a fume hood in open atmosphere (oxic) or in a

4    chamber containing $N_2$ with $H_2$ (0.7%) to maintain anoxic conditions. The aliquot samples were

5    acidified with 20 µL of 70% $HNO_3$ for analysis with inductively coupled plasma mass

6    spectroscopy (ICP-MS) for Tc and ICP optical emission spectroscopy (ICP-OES) for Cr.

7    **Reduction Capacity**: The Ce(IV) method was used to calculate reductive capacity of the KMS-2

8    and KMS-2-SS. The method has previous been reported,[39-41] and was applied here with slight

9    modifications. Here, 0.01 g aliquots of the KMS materials were placed in 15 mL of a 40 mM

10   Ce(IV) stock solution prepared with 10% $H_2SO_4$. The mixture was agitated on a mechanical

11   shaker for 72 h. Following agitation, a 5-mL aliquot was filtered with a 0.45-µm syringe filter

12   and titrated with a 20 mM $(NH_4)_2Fe(SO_4)_2$ solution using 0.05 mL of ferroine solution (Fluka) as

13   an indicator. The titration was carried out until a faint pink/blue (lilac) color was observed. The

14   reductive capacity was calculated via the difference between the oxidizing equivalents in the

15   initial Ce(IV) solution and the reducing equivalent of Fe(II) titrated to react with the excess

16   Ce(IV) remaining following reaction with the KMS-2; the reductive capacity was then corrected

17   for the mass of the sample added to the Ce(IV) solution.

18   **X-ray Diffraction:** Powders were loaded into a zero-background holder and diffraction data

19   collected with a Rigaku Miniflex II Bragg-Brentano diffractometer using Cu-Kα radiation

20   (λ = 1.5418 Å) and a graphite post-diffraction monochromator. Phases were identified by

21   comparing experimental patterns with those simulated from crystal structures using the program

22   TOPAS (v4.2, Bruker AXS). The structure for KMS-2 was obtained from Mertz et. al (2013);

1    other structures were obtained from the ICSD database (Fachinformationszentrum, Karlsruhe,

2    Germany).

3    **X-ray Absorption Spectroscopy:** X-ray absorption spectroscopy (XAS) data were obtained at

4    the Stanford Synchrotron Radiation Lightsource Beamline 11-2. The monochromator was

5    detuned 50% to reduce the harmonic content of the beam. Transmission data was obtained using

6    Ar filled ion chambers. Fluorescence data were obtained using a 100 element Ge detector and

7    have been corrected for detector dead time. Data were converted from raw data to spectra using

8    SixPack.[42] Spectra were normalized using Athena.[43] Normalized XANES spectra were fit using

9    standard spectra in the locally-written program, *fites*, which performed non-linear least squares

10   fit of the data.[44] XANES standard spectra were carefully energy calibrated using $TcO_4^-$ adsorbed

11   on Reillex-HPQ as the energy reference. The XANES spectral resolution is 7 eV based on the

12   width of the $TcO_4^-$ pre-edge peak, so each spectrum possesses 17 independent data points (range

13   of the spectrum/resolution).

14       To match  energy resolution of the $Tc_2S_7$ spectrum,, XANES spectra of the samples and of

15   the $TcO_4^-$ reference were convolved with a 1.8 eV Gaussian, and the XANES spectrum of

16   $[(EDTA)Tc(\mu\text{-}O)]_2$ ($Tc^{(IV)}EDTA$) was convolved with a 1 eV Gaussian. $Tc^{(IV)}EDTA$ is the

17   Tc(IV) reference spectrum for these samples. $TcO_2 \cdot xH_2O$ was initially used; however, the

18   spectrum of $Tc^{(IV)}EDTA$ better matches the sample XANES spectra. The main difference

19   between $TcO_2 \cdot xH_2O$ and $Tc^{(IV)}EDTA$ is that the local environment of $Tc^{(IV)}EDTA$ is more

20   distorted, which makes it a better reference standard for Tc(IV) adsorbed on a mineral surface.

21   Note that $Tc_2S_7$ is also a Tc(IV) compound, but its XANES spectrum is distinct from either

22   $TcO_2 \cdot xH_2O$ or $Tc^{(IV)}EDTA$. $Tc_2S_7$ may be better formulated as $Tc_2S(S_2)_3$ where $S_2$ is the

23   disulfide anion, $S_2^{2-}$, and the structure is given elsewhere.[45] EXAFS data were fit using Artemis

1   with theoretical scattering curves calculated with Feff 8.5 from the structures of $Tc_2S_7$ and

2   $TcO_2 \cdot xH_2O$ previously reported.

3   **Results and Discussion:**

4   ***Tc removal from DIW and LAW simulant***: Results of anoxic and oxic removal of Tc by

5   KMS-2 and KMS-2-SS in DIW and the LAW simulant batch experiments as a function of

6   contact time are presented in Figure 1. For the DIW experiments in Figure 1a, it is seen that,

7   apart from the experiment performed in oxic conditions with KMS-2, the Tc concentration

8   decreases with time. It also appears that a maximum removal value was achieved after the 14-d

9   experiment. For batch experiments at 14 d in anoxic conditions with DIW, KMS-2 removal was

10  24 µmol Tc per gram (45% of the available Tc) and KMS-2-SS removal was 50 µmol Tc per

11  gram (92% of the available Tc).
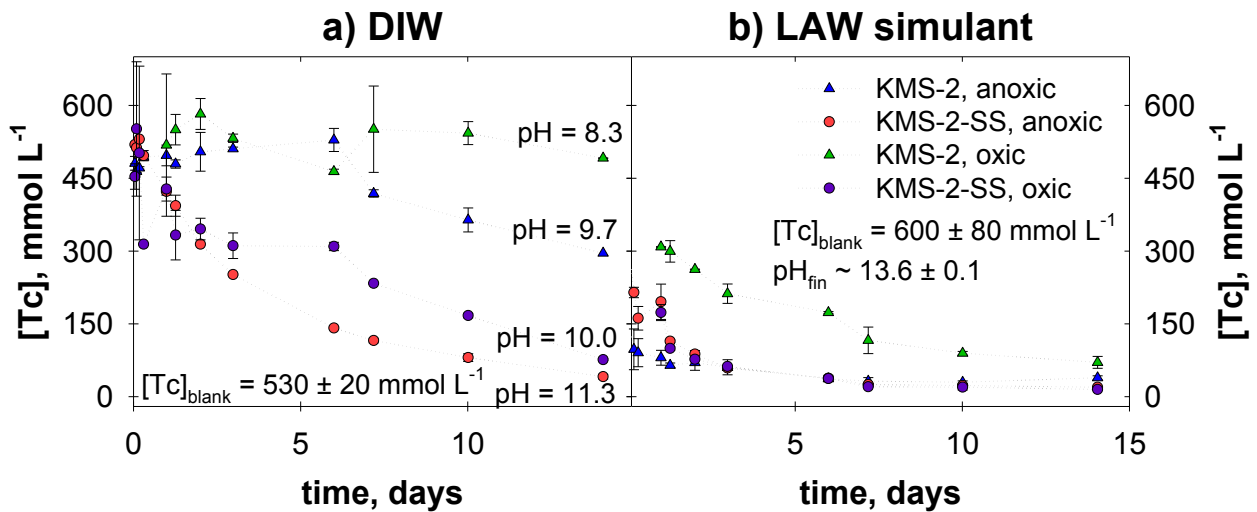


13  Figure 1 – The Tc concentration (µmol/L) as a function contact time with KMS-2 and KMS-2-SS in oxic and anoxic

14  conditions in 1) DIW and 2) the LAW simulant. The error bars (given as 1σ) are the standard deviation of the Tc

15  concentration from duplicate samples. The measured final pH presented for DIW samples is placed near the

1  experiment to which is corresponds. The pH for the LAW simulant was invariant for each experiment and is

2  presently merely as the measured average.

3  In oxic conditions, removal of Tc by KMS-2 was not measurable within error; whereas, for

4  KMS-2-SS, the Tc removal was 44 µmol Tc per gram (82% of the available Tc). Therefore, in

5  DIW, KMS-2-SS material exhibits a greater Tc removal compared with the carbonate-containing

6  KMS-2. Additional experiments, in which samples were prepared under anoxic conditions then

7  transferred to oxic conditions for 14 d, demonstrated that once Tc was removed by KMS-2 in

8  anoxic conditions, it did not release Tc upon exposure to air. This is an important result as the

9  stability of the Tc-sequestering phase, presumably $Tc_2S_7$ (see below), is an important attribute

10  for a system based on Tc(VII) reduction to less soluble Tc(IV).

11  The final pH of the system in initially DIW was measured and is presented in Figure 1a. It is

12  seen that the Tc concentration decreases with increasing solution pH. Because KMS-2-SS

13  consistently gives higher measured final pH values compared with KMS-2, a higher pH may be

14  the reason behind improved Tc removal by KMS-2-SS compared with KMS-2 in DIW. A similar

15  trend in Tc removal has also been observed, in which the removal of Tc(VII) by an FeS

16  improved with increasing pH.[28] Additionally, the higher purity of the layered material in the

17  KMS-2-SS compared with KMS-2 may also lead to a greater capacity to reduce Tc. Under

18  anoxic conditions in DIW, both KMS-2 and KMS-2-SS exhibit improved performance. This is

19  likely due to buffering and lowering of the pH in the DIW system by atmospheric $CO_2$ and

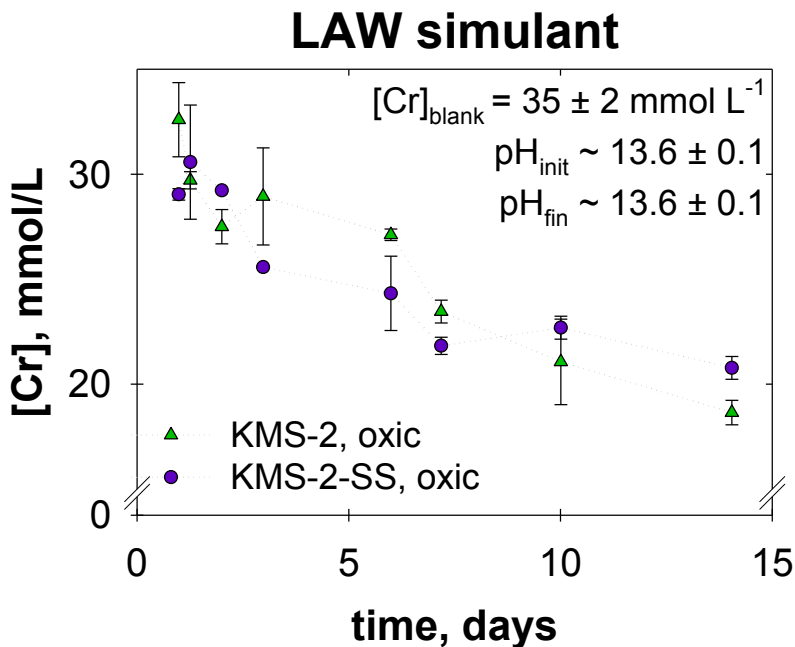20  competition between $TcO_4^-$ and $O_2$ for reduction.

21  Figure 1b presents the results from the batch sorption experiments performed in LAW

22  simulant. It can clearly be seen that the KMS-2 is more effective in the LAW solution compared

23  with the DIW solution while KMS-2-SS performs slightly better in the LAW simulant compared

11

with DIW. In anoxic conditions, KMS-2 removes 56 µmol Tc per gram (95% of the available

Tc) from the LAW simulant, and KMS-2-SS removes 59 µmol Tc per gram (97% of the

available Tc).

In oxic conditions, KMS-2 removes 52 µmol Tc per gram (88% of the available Tc), from

the LAW solution, and KMS-2-SS removes 58 µmol Tc per gram (97% of the available Tc). The

values of more than 50 µmol Tc per gram for KMS-2 in the oxic and anoxic experiments are up

to two times the removal compared with batch experiments performed in DIW. The two

properties of the LAW simulant that are attributed to the improvement in the Tc removal

efficiency of KMS-2 and KMS-2-SS are the higher pH (13.5) and high ionic strength (6 – 8 M

Na). Increasing the solution alkalinity has been shown in previous work to improve the reduction

of Tc(VII) by sulfide in solution. Increasing the ionic strength of solution has also been shown in

previous works to improve the rate and extent of Tc(VII) removal from solution.[28,46]

The results from these batch sorption tests are promising due to the Tc removal capacity of

the materials in the highly caustic, high-ionic strength LAW. In a previous study where a set of

promising Tc sequestering materials were evaluated, every sorbent except for KMS-2

experienced a large decrease in Tc removal capacity in LAW simulant compared to DIW.[47-48]

The decrease in performance by these materials in the LAW simulant was attributed to a

combination of interference from the excess Cr in the simulant solution and the high pH. The

initial Cr concentration in the LAW was measured to be $3.5 \times 10^{-2}$ M. However, the KMS-2 can

overcome the competitive Cr(VI) effect as demonstrated in Figure 2, where the removal of Cr

from LAW simulant in the oxic batch experiments is shown. At 14 d, the KMS-2 removed 1581

µmol Cr $g^{-1}$ (47% of the available Cr) and KMS-2-SS removed 1385 µmol Cr $g^{-1}$ (41% of the

1    available Cr. This change in Cr levels is also observed by the color change of the solution from

2    yellow initially due to Cr(VI) to blue at 14 d due to Cr(III).

## LAW simulant



$[Cr]_{blank}$ = 35 ± 2 mmol L$^{-1}$
$pH_{init}$ ~ 13.6 ± 0.1
$pH_{fin}$ ~ 13.6 ± 0.1

KMS-2, oxic
KMS-2-SS, oxic

3

4    Figure 2 – The Cr concentration (mmol/L) as a function contact time with KMS-2 and KMS-2-SS in oxic conditions

5    in the LAW simulant. The error bars (given as 1σ) are the standard deviation of the Cr concentration from duplicate

6    samples. The pH for the LAW simulant was invariant for each experiment and is presently merely as the measured

7    average.

8    The ability to remove both Tc and Cr is likely a result of the $S^{2-}$ content of the KMS-2 where

9    the $S^{2-}$ can reduce both Tc(VII) and Cr(VI) to Tc(IV) and Cr(III), respectively. In a measurement

10    of the reductive capacity of the KMS-2 materials, following a method similar to Um et al.,[41]

11    KMS-2 had a reductive capacity of 7.4 ± 0.6 meq g$^{-1}$ and the KMS-2-SS measured 20 ± 3 meq g$^{-}$

12    $^{1}$. These values are equivalent to removing 2.5 mmol g$^{-1}$ KMS-2 or 6.5 mmol g$^{-1}$ KMS-2-SS of

13    Tc or Cr.

1    *Change in KMS structure:* The XRD patterns for KMS-2 are presented in Figure 3 for the

2    unreacted material, the KMS-2 material after Tc removal from DIW in oxic conditions, and the

3    KMS-2 material after Tc removal from the LAW simulant in oxic conditions. The unreacted

4    material contains substantial amounts of magnesite ($MgCO_3$), schoenfliesite [$MgSn(OH)_6$], and

5    $SnO_2$. The material has a layered structure as indicated by the large peak at 8.7 Å.
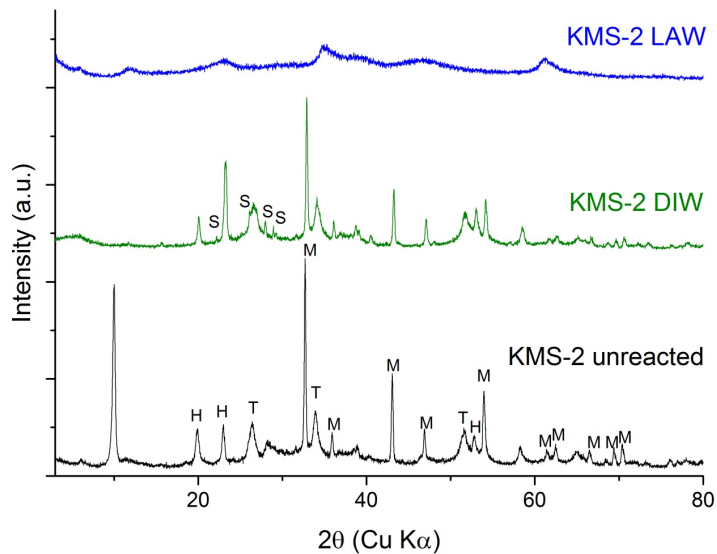


6

7    Figure 3 – X-ray diffraction patterns of starting material KMS-2 (black pattern), the KMS-2 material after Tc

8    removal from DIW in oxic conditions (green pattern), and the KMS-2 material after Tc removal from LAW

9    simulant in oxic conditions (blue pattern). The (M) indicates peaks associated with magnesite ($MgCO_3$), the (H)

10   indicates $MgSn(OH)_6$, the (T) indicates $SnO_2$, and the (S) indicates elemental Sulfur.

11       For the layered material used in the DIW experiment, the pre- and post-reaction patterns are

12   nearly identical apart from the disappearance of the peak at 8.7 Å. This would indicate that the

13   layered material is largely unaltered upon removal of $TcO_4^-$ from solution. For the sample

14   obtained from the LAW simulant experiment, compared to the largely crystalline starting

15   material, the reacted sample appears to have undergone a major structural change with only

14

1    small, broad peaks associated very small crystallites (nanoparticles). This result is in contrast to

2    previous studies on contaminant removal with KMS-2, which demonstrated ion-exchange

3    behavior where cations from solution replace $K^+$ in the interlayers on the KMS-2 structure.[29] The

4    great change in the XRD pattern after contact with the LAW simulant suggests that the structure

5    of the KMS-2 material is greatly altered during Tc removal. This alteration could be caused by

6    the loss of sulfide ions from the octahedral layers of the KMS-2.

7    *Tc oxidation state and environment in KMS:* The Tc K-edge XAS spectra of the reference

8    standards were obtained and the results are given in Figure S1 (SI). Three standard spectra were

9    used: $TcO_4^-$, $Tc_2S_7$, and $Tc^{(IV)}$EDTA complex. The latter represents Tc(IV) coordinated by

10   oxygen atoms in a distorted octahedral environment.  The bulk XANES spectra for KMS-2 and

11   KMS-2-SS samples that were used for Tc removal in anoxic DIW systems are presented in

12   Figure 4. Corresponding XANES fitting parameters are presented in Table 2. For Tc-loaded

13   KMS-2 in anoxic DIW, the major signal contribution arises from a Tc(IV) coordinated by

14   oxygen atoms with a small contribution from $TcO_4^-$, and, no $Tc_2S_7$ was observed . The KMS-2

15   had the lowest Tc removal from the DIW batch experiments, and this XANES result illustrates

16   the importance of sulfide in the immobilization of Tc by these materials. For the KMS-2-SS from

17   anoxic DIW batch experiments the contribution to the spectrum comes entirely (within error)

18   from $Tc_2S_7$. The $Tc_2S_7$ is a commonly reported compound with Tc(IV) coordinated primarily by

19   disulfide ligands.[45] The KMS-2-SS had higher Tc removal in DIW compared with KMS-2,

20   further demonstrating the importance of sulfide for Tc immobilization.

21   Table 2 – XANES fitting results for Tc in KMS-2 in various experimental conditions. The numbers in parentheses

22   are the standard deviation of the contribution of that component for the last digit. The value of p is the probability

1    that the improvement to the fit from including this spectrum is due to noise. Components with $p < 0.05$ are

2    significant at the $2\sigma$ level and those with $p < 0.01$ are significant at the $3\sigma$ level.

| Material | Solution | Conditions | $TcO_4^-$ | p | Tc(IV) | p | $Tc_2S_7$ | p |
|---|---|---|---|---|---|---|---|---|
| KMS-2 | DIW | anoxic | 0.09(2) | 0.123 | 0.95(4) | <0.001 | 0.00(7) | 1 |
| KMS-2-SS | DIW | anoxic | 0.00(1) | 1 | 0.00(2) | 1 | 1.00(3) | <0.001 |
| KMS-2-SS | DIW | anoxic to oxic | 0.00(2) | 1 | 0.03(3) | 1 | 0.97(4) | <0.001 |
| KMS-2 | LAW simulant | anoxic | 0.00(1) | 1 | 0.01(2) | 1 | 0.99(3) | <0.001 |
| KMS-2 | LAW simulant | oxic | 0.25(2) | <0.001 | 0.12(3) | <0.001 | 0.64(3) | <0.001 |

3        The $Tc_2S_7$ that was formed in the anoxic DIW experiment with KMS-2-SS showed high

4    stability upon exposure to an oxic environment. Figure 4 displays the XANES spectrum and

5    resulting fits from KMS-2-SS that were collected from a batch experiment where the container

6    was transferred to an oxic environment after 14 d of contact in anoxic conditions. Following

7    exposure to oxic conditions, the $Tc_2S_7$ remained the only Tc species observed by XANES.
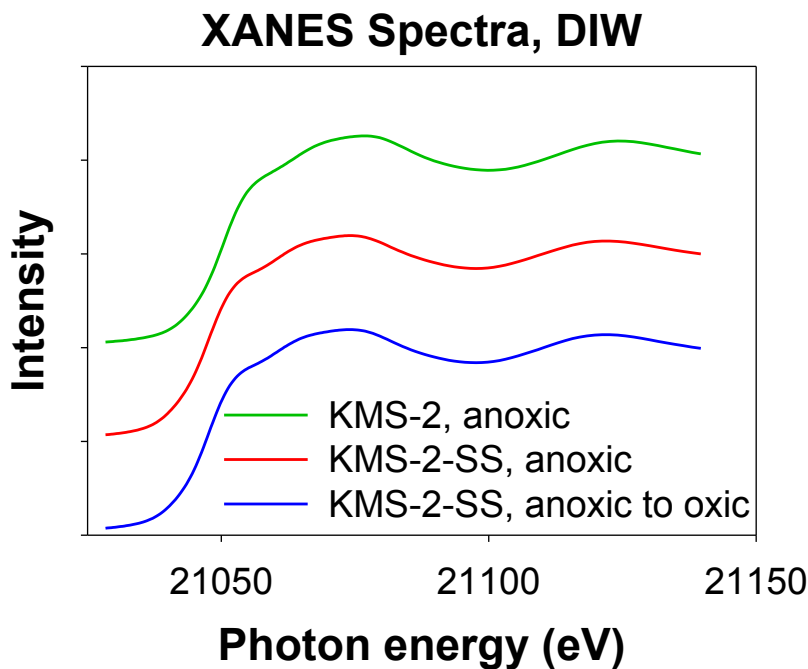


**XANES Spectra, DIW**

8

1     Figure 4 – Technetium XANES spectra of Tc in the following batch experiments: KMS-2 in DIW and anoxic

2     conditions, KMS-2-SS in DIW and anoxic conditions, and KMS-2-SS in DIW and anoxic conditions followed by

3     oxic conditions.

4        In addition to the major differences that may be observed from the XANES spectra, the local

5     environment of Tc in these samples was determined by EXAFS. The Tc K-edge EXAFS data are

6     presented for selected samples in Figure 5. For the KMS-2 sample in anoxic conditions in DIW,

7     the data are consistent with Tc-S and Tc-Tc distances suggest the presence of $Tc_2S_7$.[45] In

8     addition, a small amount of $TcO_4^-$ is present in this sample. For the KMS-2-SS samples from the

9     anoxic and anoxic-to-oxic conditions, the EXAFS spectra and fit parameters are nearly identical.

10    The interatomic distances are slightly different from those previously reported for $Tc_2S_7$, Tc-S =

11    2.378(2) Å and Tc-Tc = 2.774(2) Å.[45] The local environment of Tc is identical to that in $Tc_2S_7$

12    within error. In general, the KMS materials appear to act as a source for sulfide to reduce $TcO_4^-$

13    and precipitate it as $Tc_2S_7$, which is stable in oxic conditions, at least over short time periods.



14
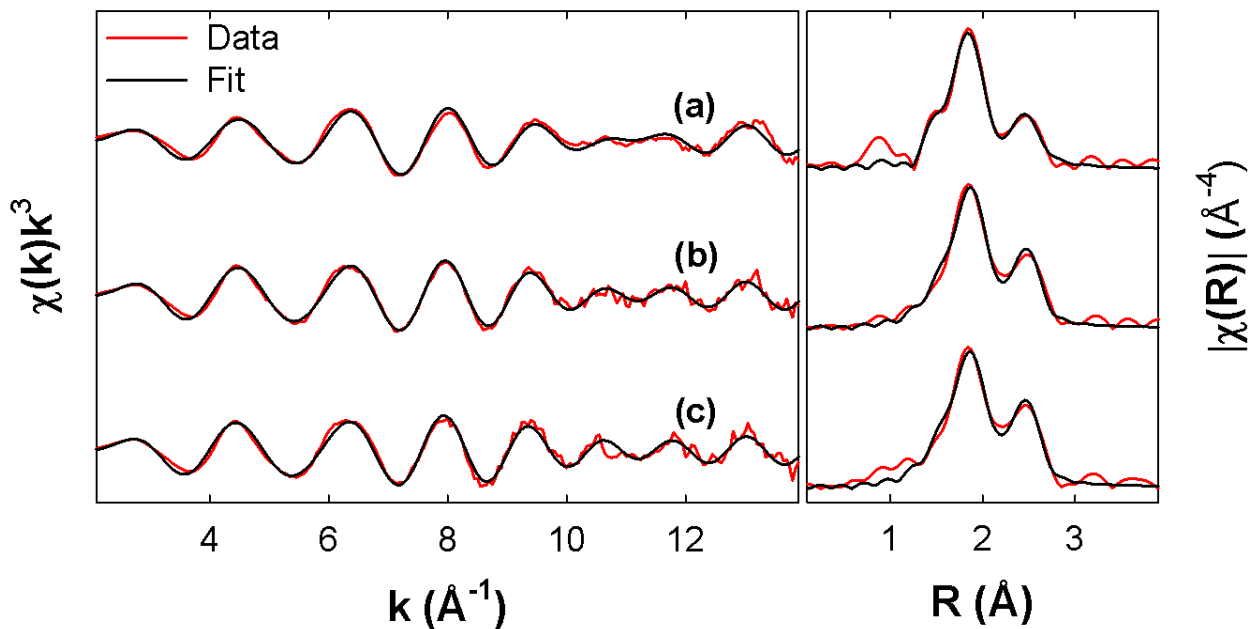
Figure 5 - EXAFS spectrum (red) and fit (black) (left panel) and Fourier Transform (right panel) for (a) KMS-2 (anoxic, DIW), (b) KMS-2-SS (anoxic, DIW), and (c) KMS-2-SS (anoxic, exposed to air, DIW). Fitting parameters are given in Table 3.|

Table 3 - EXAFS Fitting parameters for Figure 5.

| Material | Neighbor | # of Neighbors | Distance (Å) | $\sigma^2$ (Å$^2$) | p[a] | Tc$_2$S$_7$[45] |
|---|---|---|---|---|---|---|
| KMS-2 (anoxic, DIW) | O | 0.3(2) | 1.69(4) | 0.003$^c$ | 0.327 | -- |
|  | S | 4.8(7) | 2.336(9) | 0.006(1) | <0.001 | 7.4 S at 2.39 Å |
|  | Tc | 1.1(5) | 2.773(9) | 0.003(2) | 0.001 | 1.8 Tc at 2.77 Å |
| KMS-2-SS (anoxic, DIW) | S | 5.9(7) | 0.0076(9) | 2.359(7) | <0.001 | -- |
|  | Tc | 1.6(5) | 0.004(1) | 2.785(6) | <0.001 | -- |
| KMS-2-SS (anoxic, exposed to air, DIW) | S | 6.2(8) | 0.008(1) | 2.36(1) | <0.001 |  |
|  | Tc | 1.8(6) | 0.004(1) | 2.784(7) | <0.001 |  |

a) The value of p is the probability that the improvement to the fit from including this spectrum is due to noise. Components with $p < 0.05$ are significant at the 2$\sigma$ level and those with $p < 0.01$ are significant at the 3$\sigma$ level

Bulk XANES spectra were also obtained for KMS-2 from batch experiments performed in anoxic and oxic conditions with the LAW simulant are presented in Figure 6 with the results of the XANES fitting presented in Table 2. Both the spectra from the anoxic and oxic KMS-2 experiments show fits in excellent agreement with the data from the standards. The KMS-2 from the anoxic LAW simulant experiment consists primarily of a Tc$^{(IV)}_2$S$_7$ species (Figure 6a). However, as seen in Table 2 and Figure 6b, for the KMS-2 sample from the LAW simulant batch experiment performed in oxic conditions, 64% of the Tc contribution is Tc$^{(IV)}_2$S$_7$, 12% of the contribution is from Tc(IV) coordinated by oxygen atoms, and 25% is unreduced Tc$^{(VII)}$O$_4^-$. These data suggest that effective removal of Tc is possible by KMS-2 in oxidizing conditions, although the reduction reaction from the highly soluble Tc(VII) to the sparingly soluble Tc(IV) may not proceed as quickly as when Tc removal is performed in anoxic conditions due to either

1 competition between $TcO_4^-$ and $O_2$ for reduction by sulfide or due to oxidation of the sulfide

2 ligands of $Tc_2S_7$ to yield Tc(IV) species. The EXAFS analyses were not performed on the LAW

3 simulant samples. Data were not obtained from KMS-2-SS samples used for Tc removal from

4 the LAW simulant.
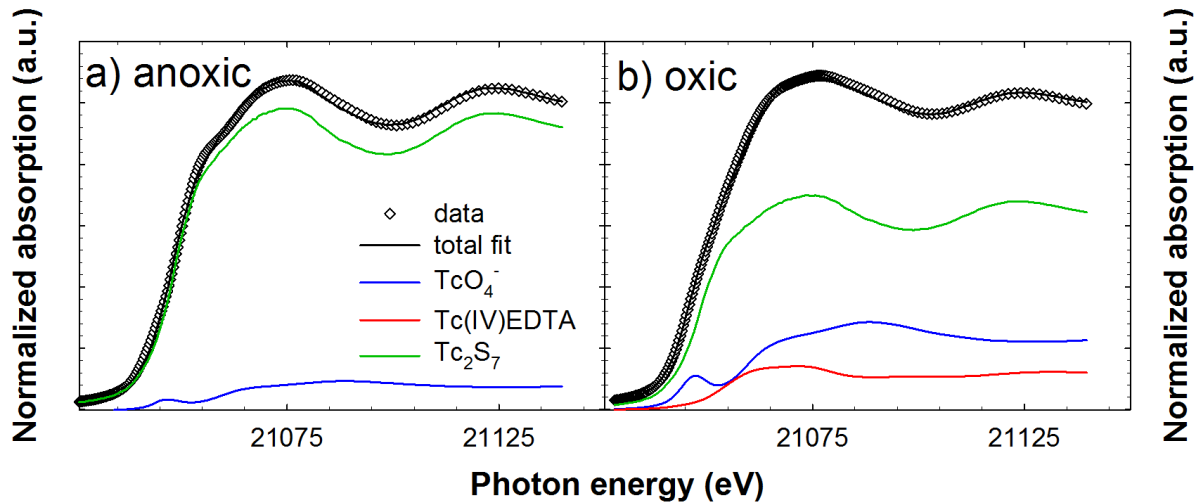


5

6 Figure 6 – Technetium XANES spectra for fits of Tc in the following batch experiments of a) KMS-2 in LAW and

7 anoxic conditions, and b) KMS-2 in LAW and oxic conditions.

**Conclusions:**

9     The KMS-2 and KMS-2-SS were successful in removing Tc(VII) from a high ion strength,

10 high pH LAW simulant. The Tc(VII) removal from LAW was improved compared with Tc

11 removal from DIW. The ability of the sulfide-containing material to remove Tc increases with

12 increasing pH and ionic strength. This property is unique among Tc sequestering materials where

13 performance is general worse in the highly caustic, high ionic strength LAW simulant. The XRD

14 analyses of the reacted material show that contact with Tc containing LAW greatly alters its

15 structure. XRD patterns of samples that were used to remove Tc from the LAW displayed broad,

1  diffuse peaks. This result indicates that the Tc removal mechanism is not a simple ion exchange

2  in the inner layer of KMS-2. *Ex-situ* spectroscopic analyses showed that Tc is mainly present in

3  the reduced Tc(IV) state in both KMS materials performed in DIW and LAW in anoxic

4  environments. The $Tc_2S_7$ species formed by the reduction of Tc(VII) by KMS-2-SS was found to

5  be stable upon exposure to oxic conditions, with limited to no re-oxidation observed over 14

6  days. In the LAW solution, KMS-2 converted Tc(VII) to $Tc^{(IV)}_2S_7$ in anoxic conditions; however,

7  the transition was less extensive in oxic conditions, with some Tc(VII) still present following the

8  batch experiments. The Tc may enter the KMS-2 as $TcO_4^-$ after which it is reduced to a Tc(IV)

9  species coordinated by various oxygen and sulfide groups depending on the availability of

10  sulfide. We note that other cations may interfere with KMS-2 functionality if they replace the K

11  in the interlayer. Further work needs to be performed to ensure that Tc(IV) reduced by layered

12  KMS-2 is not quickly reoxidized to soluble Tc(VII) and a suitable host matrix for the long-term

13  isolation of Tc-containing KMS materials needs to be found.

# 1  Figures and Tables

2

1    **References:**

2    1.      Kershaw, P. J.; McCubbin, D.; Leonard, K. S., Continuing Contamination of North Atlantic and
3    Arctic Waters by Sellafield Radionuclides. *Science of The Total Environment* **1999,** *237–238*, 119-132.
4    2.      Icenhower, J. P.; Qafoku, N. P.; Zachara, J. M.; Martin, W. J., The Biochemistry of Technetium:
5    A Review of the Behavior of an Artificial Element in the Natural Environment. *American Journal of*
6    *Science* **2010,** *310*, 721-752.
7    3.      Darab, J. G.; Smith, P. A., Chemistry of Technetium and Rhenium Species During Low-Level
8    Radioactive Waste Vitrification. *Chem. Mater.* **1996,** *8*, 1004-1021.
9    4.      Westsik Jr, J. H. *Hanford Site Secondary Waste Roadmap*; PNNL-18196; Pacific Northwest
10   National Laboratory: Richland, WA, USA, 2009.
11   5.      McCloy, J. S., et al., Rhenium Solubility in Borosilicate Nuclear Waste Glass: Implications for
12   the Processing and Immobilization of Technetium-99. *Environmental Science & Technology* **2012,** *46*,
13   12616-12622.
14   6.      Soderquist, C. Z.; Schweiger, M. J.; Kim, D.-S.; Lukens, W. W.; McCloy, J. S., Redox-
15   Dependent Solubility of Technetium in Low Activity Waste Glass. *J. Nucl. Mater.* **2014,** *449*, 173-180.
16   7.      Gong, C.-M. S.; Lukens, W. W.; Poineau, F.; Czerwinski, K. R., Reduction of Pertechnetate by
17   Acetohydroxamic Acid: Formation of Tc-Ii(No)(Aha)(2)(H2o)(+) and Implications for the Urex Process.
18   *Inorg. Chem.* **2008,** *47*, 6674-6680.
19   8.      Gawenis, J. A.; Holman, K. T.; Atwood, J. L.; Jurisson, S. S., Extraction of Pertechnetate and
20   Perrhenate from Water with Deep-Cavity Cpfe(Arene)(+)-Derivatized Cyclotriveratrylenes. *Inorg. Chem.*
21   **2002,** *41*, 6028-6031.
22   9.      Delcul, G. D.; Bostick, W. D.; Trotter, D. R.; Osborne, P. E., Tc-99 Removal from Process
23   Solutions and Contaminated Groundwater. *Separation Science and Technology* **1993,** *28*, 551-564.
24   10.     Delcul, G. D.; Bostick, W. D., Simple Method for Technetium Removal from Aqueous-Solutions.
25   *Nucl. Technol.* **1995,** *109*, 161-162.
26   11.     Milutinović-Nikolić, A.; Maksin, D.; Jović-Jovičić, N.; Mirković, M.; Stanković, D.; Mojović, Z.;
27   Banković, P., Removal of [99]tc(Vii) by Organo-Modified Bentonite. *Applied Clay Science* **2014,** *95*, 294-
28   302.
29   12.     Li, D.; Kaplan, D. I.; Knox, A. S.; Crapse, K. P.; Diprete, D. P., Aqueous [99]tc, [129]i and [137]cs
30   Removal from Contaminated Groundwater and Sediments Using Highly Effective Low-Cost Sorbents.
31   *Journal of Environmental Radioactivity* **2014,** *136*, 56-63.
32   13.     Meyer, R. E.; Arnold, W. D.; Case, F. I. *The Solubility of Electrodeposited Tc(Iv) Oxides*; ORNL-
33   6374; Oak Ridge National Laboratory: Oak Ridge, TN, 1987.
34   14.     Rard, J.; Rand, M.; Anderegg, G.; H, W., Chemical Thermodynamics of Technetium. In
35   *Chemical Thermodynamics*, Sandino, M.; Osthols, E., Eds. Elsevier: Amsterdam, 1999; Vol. 3.
36   15.     Pierce, E. M.; Serne, R. J.; Um, W.; Mattigod, S. V.; Icenhower, J. P.; Qafoku, N. P.; Westsik Jr,
37   J. H.; Scheele, R. D. *Review of Potential Candidate Stabilization Technologies for Liquid and Solid*
38   *Secondary Waste Streams*; Pacific Northwest National Laboratory: Richland, WA, January 2010, 2010.
39   16.     Wellman, D. M.; Mattigod, S. V.; Parker, K. E.; Heald, S. M.; Wang, C. M.; Fryxell, G. E.,
40   Synthesis of Organically Templated Nanoporous Tin(Ii/Iv) Phosphate for Radionuclide and Metal
41   Sequestration. *Inorg. Chem.* **2006,** *45*, 3826-3826.
42   17.     Shkrob, I. A.; Marin, T. W.; Stepinski, D. C.; Vandegrift, G. F.; Muntean, J. V.; Dietz, M. L.,
43   Extraction and Reductive Stripping of Pertechnetate from Spent Nuclear Fuel Waste Streams. *Separation*
44   *Science and Technology* **2011,** *46*, 357-368.
45   18.     Liang, L.; Gu, B.; Yin, X., Removal of Technetium-99 from Contaminated Groundwater with
46   Sorbents and Reductive Materials. *Separations Technology* **1996,** *6*, 111-122.
47   19.     Darab, J. G., et al., Removal of Pertechnetate from Simulated Nuclear Waste Streams Using
48   Supported Zerovalent Iron. *Chem. Mater.* **2007,** *19*, 5703-5713.

20.	Fan, D., et al., Reductive Sequestration of Pertechnetate ($^{99}$tco$_4^-$) by Nano Zerovalent Iron (Nzvi) Transformed by Abiotic Sulfide. *Environmental Science & Technology* **2013,** *47*, 5302-5310.

21.	Watson, J. H. P.; Ellwood, D. C., The Removal of the Pertechnetate Ion and Actinides from Radioactive Waste Streams at Hanford, Washington, USA and Sellafield, Cumbria, Uk: The Role of Iron-Sulfide-Containing Adsorbent Materials. *Nuclear Engineering and Design* **2003,** *226*, 375-385.

22.	Mattigod, S. V.; Westsik Jr, J. H.; Wellman, D., M., Evaluation and Selection of $^{99}$tc Getters for Sequestration of Liquid Secondary Waste Resulting from Vitrification of Radioactive Wastes from Hanford. In *WM2011 Conference*, Phoenix, Arizona, 2011.

23.	Riley, B. J.; Chun, J.; Um, W.; Lepry, W. C.; Matyas, J.; Olszta, M. J.; Li, X.; Polychronopoulou, K.; Kanatzidis, M. G., Chalcogen-Based Aerogels as Sorbents for Radionuclide Remediation. *Environmental Science & Technology* **2013,** *47*, 7540-7547.

24.	Gu, B.; Dowlen, K. E.; Liang, L.; Clausen, J. L., Efficient Separation and Recovery of Technetium-99 from Contaminated Groundwater. *Separations Technology* **1996,** *6*, 123-132.

25.	Wang, Y.; Gao, H.; Yeredla, R.; Xu, H.; Abrecht, M., Control of Pertechnetate Sorption on Activated Carbon by Surface Functional Groups. *J. Colloid Interface Sci.* **2007,** *305*, 209-217.

26.	Petrovic, D.; Dukic, A.; Kumric, K.; Babic, B.; Momcilovic, M.; Ivanovic, N.; Matovic, L., Mechanism of Sorption of Pertechnetate onto Ordered Mesoporous Carbon. *J. Radioanal. Nucl. Chem.* **2014,** *302*, 217-224.

27.	Galambos, M.; Dano, M.; Viglasova, E.; Krivosudsky, L.; Rosskopfova, O.; Novak, I.; Berek, D.; Rajec, P., Effect of Competing Anions on Pertechnetate Adsorption by Activated Carbon. *J. Radioanal. Nucl. Chem.* **2015,** *304*, 1219-1224.

28.	Liu, Y.; Terry, J.; Jurisson, S. S., Pertechnetate Immobilization in Aqueous Media with Hydrogen Sulfide under Anaerobic and Aerobic Environments. *Radiochimica Acta* **2007,** *95*, 717-725.

29.	Mertz, J. L.; Fard, Z. H.; Malliakas, C. D.; Manos, M. J.; Kanatzidis, M. G., Selective Removal of Cs$^+$, Sr$^{2+}$, and Ni$^{2+}$ by K$_{2x}$mg$_x$sn$_{3-X}$S$_6$ (X = 0.5–1) (Kms-2) Relevant to Nuclear Waste Remediation. *Chem. Mater.* **2013,** *25*, 2116-2127.

30.	Fard, Z. H.; Malliakas, C. D.; Mertz, J. L.; Kanatzidis, M. G., Direct Extraction of Ag$^+$ and Hg$^{2+}$ from Cyanide Complexes and Mode of Binding by the Layered K$_2$mgsn$_2$s$_6$ (Kms-2). *Chem. Mater.* **2015,** *27*, 1925-1928.

31.	Manos, J. M.; Ding, N.; Kanatzidis, M. G., Layered Metal Sulfides: Exceptionally Selective Agents for Radioactive Strontium Removal. *Proceedings of the National Academy of Sciences* **2008,** *150*, 3696-3699.

32.	Manos, M. J.; Kanatzidis, M. G., Layered Metal Sulfides Capture Uranium from Seawater. *J. Am. Chem. Soc.* **2012,** *134*, 16441-16446.

33.	Sarma, D.; Malliakas, C. D.; Subrahmanyam, K. S.; Islam, S. M.; Kanatzidis, M. G., K$_{2x}$sn$_{4-X}$s$_{8-X}$ (X = 0.65-1): A New Metal Sulfide for Rapid and Selective Removal of Cs$^+$, Sr$^{2+}$ and Uo$_2^{2+}$ Ions. *Chemical Science* **2016,** *7*, 1121-1132.

34.	Asmussen, R. M.; Neeway, J. J.; Lawter, A. R.; Levitskaia, T. G.; Lukens, W. W.; Qafoku, N. P., The Function of Sn(Ii)-Apatite as a $^{99}$tc Immobilizing Agent. *submitted to Environmetal Science & Technology* **2016**.

35.	Asmussen, R. M.; Neeway, J. J.; Qafoku, N. P. In *Technetium and Iodine Getters to Improve Cast Stone Performance – 15420*, WM2015 Conference, Phoenix, AZ, USA, March 15-19, 2015; Phoenix, AZ, USA, 2015.

36.	Neeway, J. J.; Lawter, A. J.; Serne, R. J.; Asmussen, R. M.; Qafoku, N. P. In *Technetium Getters to Improve Cast Stone Performance*, Scientific Basis for Nuclear Waste Management XXXVIII, Boston, Massachusetts, Gin, S.; Jubin, R.; Matyas, J.; Vance, E., Eds. Materials Research Society: Boston, Massachusetts, 2015.

37.	Fan, D.; Anitori, R. P.; Tebo, B. M.; Tratnyek, P. G.; Lezama Pacheco, J. S.; Kukkadapu, R. K.; Kovarik, L.; Engelhard, M. H.; Bowden, M. E., Oxidative Remobilization of Technetium Sequestered by Sulfide-Transformed Nano Zerovalent Iron. *Environmental Science & Technology* **2014,** *48*, 7409-7417.

1    38.    Russel, R. L.; Westsik Jr, J. H.; Swanberg, D. J.; Eibling, R. E.; Cozzi, A.; Lindberg, M. J.;
2    Josephson, G. B.; Rinehart, D. E. *Letter Report: Law Simulant Development for Cast Stone Screening*
3    *Tests*; PNNL-22352; Pacific Northwest National Laboratory: Richland, WA, 2013.
4    39.    Angus, M. J.; Glasser, F. P. In *The Chemical Environment in Cement Matrices*, Scientific Basis
5    for Nuclear Waste Management IX, Stockholm, Sweden, Werme, L., Ed. Materials Research Society:
6    Stockholm, Sweden, 1985; pp 547-553.
7    40.    Kaplan, D. I.; Hang, T.; Aleman, S. E. *Estimated Duration of the Reduction Capacity within a*
8    *High-Level Waste Tank*; WSRC-RP-2005-01674; Westinghouse Savannah River Company: Aiken, SC,
9    2005.
10   41.    Um, W.; Yang, J.-S.; Serne, R. J.; Westsik, J. H., Reductive Capacity Measurement of Waste
11   Forms for Secondary Radioactive Wastes. *J. Nucl. Mater.* **2015,** *467*, 251-259.
12   42.    Webb, S. M., Sixpack: A Graphical User Interface for Xas Analysis Using Ifeffit. *Phys. Scr.*
13   **2005,** *T115*, 1011-1014.
14   43.    Ravel, B.; Newville, M., Athena and Artemis: Interactive Graphical Data Analysis Using Ifeffit.
15   *Phys. Scr.* **2005,** *T115*, 1007-1010.
16   44.    http://lise.lbl.gov/RSXAP.
17   45.    Lukens, W. W.; Bucher, J. J.; Shuh, D. K.; Edelstein, N. M., Evolution of Technetium Speciation
18   in Reducing Grout. *Environmental Science & Technology* **2005,** *39*, 8064-8070.
19   46.    Lieser, K. H.; Bauscher, C., Technetium in the Hydrosphere and in the Geosphere. *Radiochimica*
20   *Acta* **1987,** *42*, 205-214.
21   47.    Qafoku, N. P.; Neeway, J. J.; Lawter, A. R.; Levitskaia, T. G.; Serne, R. J.; Westsik Jr, J. H.;
22   Valenta Snyder, M. M. *Technetium and Iodine Getters to Improve Cast Stone Performance*; PNNL-
23   23282; Pacific Northwest National Laboratory: Richland, WA, 2014.
24   48.    Neeway, J. J.; Qafoku, N. P.; Serne, R. J.; Lawter, A. R.; Stephenson, J. R.; Lukens, W. W.;
25   Westsik Jr, J. H. *Evaluation of Technetium Getters to Improve the Performance of Cast Stone*; PNNL-
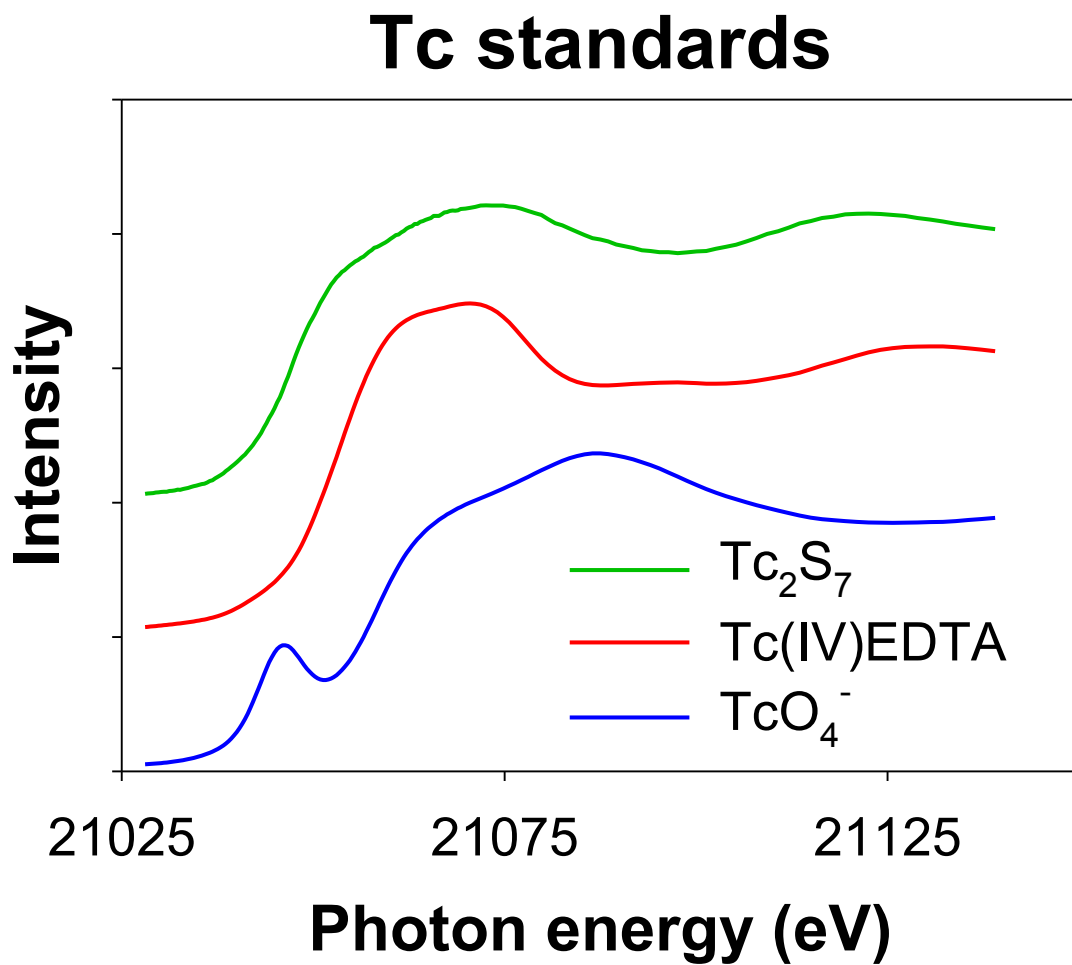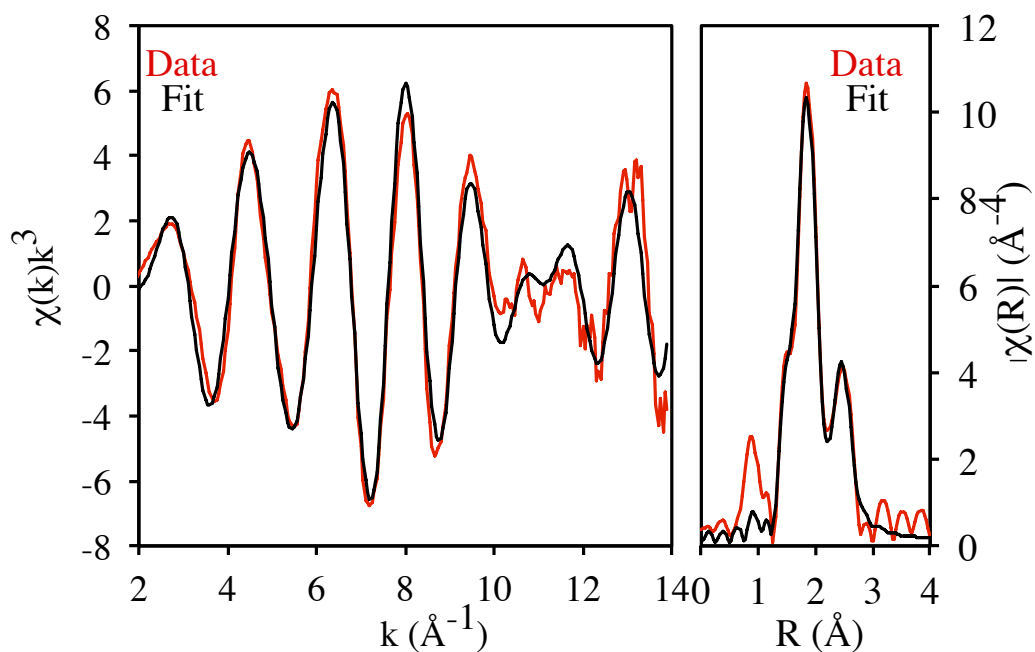26   23667; Pacific Northwest National Laboratory: Richland, WA, 2014.

27

28

1    Supporting Information

2

# Tc standards



Intensity

Tc$_2$S$_7$

Tc(IV)EDTA

TcO$_4^-$

21025          21075          21125

# Photon energy (eV)

3

4          **Figure S1.** Technetium XANES Tc standard spectra used for fitting.

5

**Figure S2. KMS-2 (anoxic, DIW) EXAFS spectrum (red) and fit (black) (left panel) and its Fourier Transform (right panel). Fitting parameters are given in Table S1.**

**Table S1. EXAFS Fitting parameters for Figure S2.**

| Neighbor | # of Neighbors | Distance (Å) | $\sigma^2$ (Å$^2$) | p | $Tc_2S_7$[b] |
|:---:|:---:|:---:|:---:|:---:|:---:|
| *O* | 0.3(2) | 1.69(4) | 0.003[c] | 0.327 | -- |
| *S* | 4.8(7) | 2.336(9) | 0.006(1) | <0.001 | 7.4 S at 2.39 Å |
| *Tc* | 1.1(5) | 2.773(9) | 0.003(2) | 0.001 | 1.8 Tc at 2.77 Å |

a) $S_0^2$=0.8 (fixed), $\Delta E$= 3(2) eV;
b) Lukens, W. W.; Bucher, J. J.; Shuh, D. K. Edelstein, N. M.; *Env. Sci. Tech.* **2005**, *39*, 8064.
c) Parameter fixed at this value

1



2
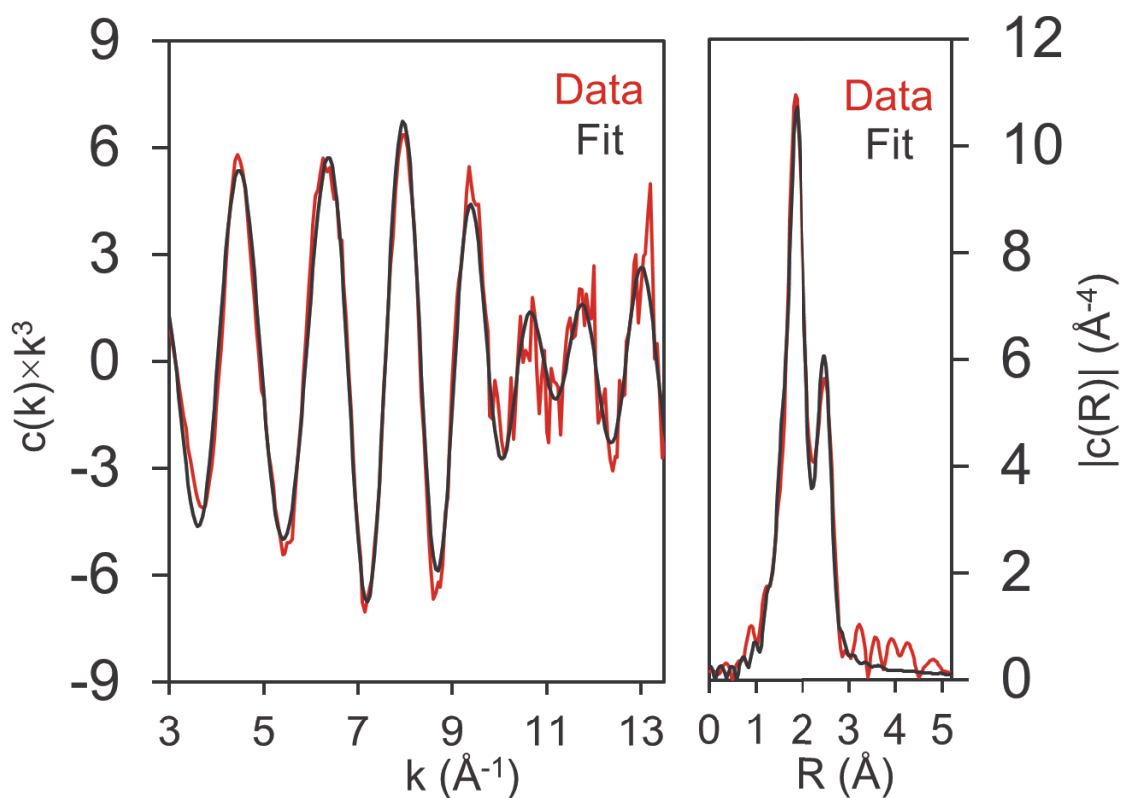
**Figure S3. KMS-2-SS (anoxic, DIW) EXAFS spectrum (red) and fit (black) (left panel) and its Fourier Transform (right panel). Fitting parameters are given in Table S2.**

5

**Table S2. EXAFS Fitting parameters for Figure S3.**

| Neighboring Atom | # of Neighbors | $\sigma^2$ ($\text{Å}^2$) | Distance (Å) | $p^b$ |
|---|---|---|---|---|
| S | 5.9(7) | 0.0076(9) | 2.359(7) | <0.001 |
| Tc | 1.6(5) | 0.004(1) | 2.785(6) | <0.001 |

a)  Fit range: 2<k<14, 1<R<3; 16.9 independent data. 7 parameters, $S_0^2 = 0.8$ $\Delta E_0 = 5(1)$ eV, $\chi^2 = 106$, $\chi_v^2 = 13$, R = 0.013.

b)  The value of p is the probability that the improvement to the fit from including this spectrum is due to noise. Components with p < 0.05 are significant at the $2\sigma$ level and those with p < 0.01 are significant at the $3\sigma$ level.
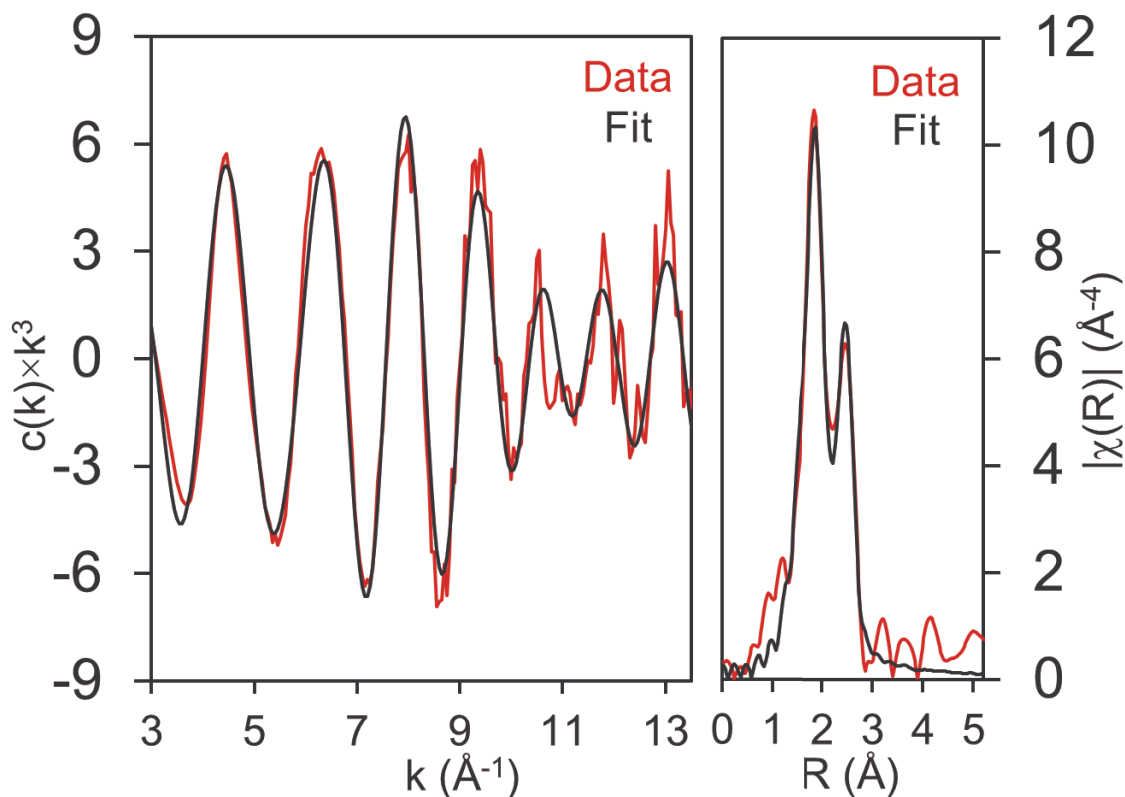
**Figure S4. KMS-2-SS (anoxic, exposed to air, DIW) EXAFS spectrum (red) and fit (black) (left panel) and its Fourier Transform (right panel). Fitting parameters are given in Table S3.**

**Table S3: Best fit parameters for KMS-2-SS-DI (Ch to FH)**

| Neighboring Atom | # of Neighbors | $\sigma^2$ ($\text{Å}^2$) | Distance (Å) | $p^b$ |
|---|---|---|---|---|
| S | 6.2(8) | 0.008(1) | 2.36(1) | <0.001 |
| Tc | 1.8(6) | 0.004(1) | 2.784(7) | <0.001 |

a)  Fit range: $2<k<14$, $1<R<3$; 16.9 independent data. 7 parameters, $S_0^2 = 0.8$, $\Delta E_0 = 4(1)$ eV, $\chi^2 = 187$, $\chi_v^2 = 23.6$, R = 0.020.

b)  The value of p is the probability that the improvement to the fit from including this spectrum is due to noise. Components with $p < 0.05$ are significant at the $2\sigma$ level and those with $p < 0.01$ are significant at the $3\sigma$ level.